JACS
JOURNAL OF THE AMERICAN CHEMICAL SOCIETY
Article
pubs.acs.org/JACS

Key Structural Motifs To Predict the Cage Topology in Endohedral Metallofullerenes

Yang Wang,*[†,‡] Sergio Díaz-Tendero,[†,§] Fernando Martín,[†,‡,§] and Manuel Alcamí[†,‡]

[†]Departamento de Química, Módulo 13, Universidad Autónoma de Madrid, 28049 Madrid, Spain
[‡]Instituto Madrileño de Estudios Avanzados en Nanociencia (IMDEA-Nanociencia), Cantoblanco, 28049 Madrid, Spain
[§]Condensed Matter Physics Center (IFIMAC), Universidad Autónoma de Madrid, 28049 Madrid, Spain

Supporting Information

ABSTRACT: We show that the relative isomer stability of fullerene anions is essentially governed by a few simple structural motifs, requiring only the connectivity information between atoms. Relative energies of a large number of isomers of fullerene anions, C_{2n}^{q} ($2n$ = 68−104; q = −2, −4, −6), can be satisfactorily reproduced by merely counting the numbers of seven kinds of hexagon-based motifs. The dependence of stability on these motifs varies with the charge state, which reflects the fact that the isomeric form of the carbon cage in endohedral metallofullerenes (EMFs) often differs from that in neutral empty fullerenes. The chemical origin of the stabilization differences between motifs is discussed on the basis of electronic and strain effects as well as aromaticity. On the basis of this simple model, the extraordinary abundance of the icosahedral C_{80} cage in EMFs can be easily understood. We also provide an explanation for why the well-known isolated pentagon rule is often violated in smaller EMFs. Finally, simple topological indices are proposed for quantitatively predicting the relative stability of fullerene anions, allowing a rapid determination of suitable hosting cages in EMFs by just counting three simple structural motifs.

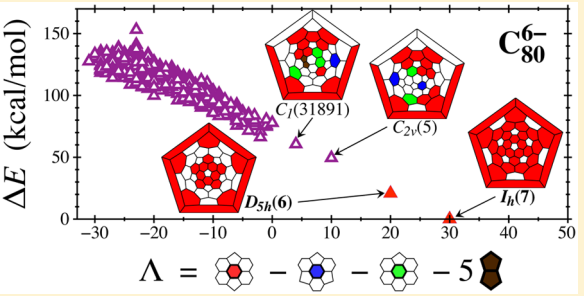

1. INTRODUCTION

Endohedral metallofullerenes (EMFs)[1,2] are a new family of hybrid compounds comprising a fullerene cage encapsulating a metal atom or a metal-containing cluster. They have attracted considerable attention in the last two decades, because of their unique properties[3] with promising applications, especially in biomedicine[4−6] and photovoltaics.[7,8] In recent years, the study of EMFs is booming owing to the increasing amount of successful production and isolation of these compounds.[1,2,9−15] Compared to the very limited number of isolated and identified empty fullerenes (such as C_{60}, C_{70}, C_{76}, C_{78}, C_{82}, C_{84}),[16] a wide range of fullerenes with different sizes (from C_{28}[17] to C_{104}[18]) and isomeric forms have been isolated as the hosting cages in EMFs.[1,2,19,20] Among them, the isomeric cage structures of EMFs ranging from C_{66}[10,21,22] to C_{104}[18] have been unambiguously identified in experiments.[1]

The encapsulation of metal species into the carbon cage not only enriches the variety of isolable fullerenes, but also changes the isomeric form of the cages in existence. Taking fullerene C_{78} as an example, the isolated empty cages correspond to isomers with D_3 and C_{2v} symmetries,[23−25] while when isolated in the form of EMFs (encapsulating, e.g., La_2, Ce_2, Ti_2C_2 or Sc_3N) the cage corresponds to an isomer with D_{3h} symmetry.[1,2] An interesting observation in this respect is that the well-accepted isolated pentagon rule (IPR)[26] for the stability of neutral empty fullerenes is often violated in EMFs with cages smaller than C_{86}.[27,28]

In order to understand the stability of EMFs, some theoretical attempts have been made during the past decade.[1,27] First of all, it is well-established that the relative stability of cage isomers in EMFs is usually the same as that of the isomers of empty fullerene anions in the appropriate charge states.[1,28] This implies that the metal-cage interaction can be conveniently replaced by a formal charge transfer to the cage, provided that the sizes of the cage and the encapsulated species are compatible. The latter can be predicted by a simple spacing filling model.[29] This simplified yet effective ionic cage model reduces the complexity of the problem. However, there is still a huge number of isomers to consider in the search for suitable cages in EMFs. Although extensive semiempirical computations may be feasible nowadays to routinely predict the most stable fullerene anions, new chemical insights and concepts are required to better understand the underlying factors governing the stability of these charged fullerenes. In 2005, Poblet et al.[30] suggested that the fullerene isomers with the largest gaps between LUMO+2 and LUMO+3 (or LUMO+1 and LUMO +2) should be the preferable hosts for the molecules or clusters that formally transfer six[30] (or four[31]) electrons. Zettergren et al.[32] proposed that more stable fullerene anions should have a more uniform distribution of adjacent pentagon pairs (APPs) and pyrene motifs, as in this way the Coulomb repulsion between the charges located at these motifs is minimized. Later

Received: October 9, 2015
Published: January 13, 2016

DOI: 10.1021/jacs.5b10591
J. Am. Chem. Soc. 2016, 138, 1551−1560

on, based on similar electrostatic arguments, Poblet et al.[33] quantified the distribution of pentagons by defining the inverse pentagon separation index (IPSI) calculated from the geometry of a fullerene cage. Some correlations between the IPSI and the relative energy of isomers have been shown in fullerene hexaanions and tetraanions.[33,34] Alternatively, Solà et al.[35,36] suggested that the total aromaticity is the main stabilizing factor for fullerene anions.

Almost all the above-mentioned prediction tools, however, require the knowledge of optimized geometries based on density functional theory (DFT) or at least semiempirical quantum chemistry calculations. This is not convenient for practical use, especially for studying relatively large-sized fullerenes with a great number of isomers to consider. For example, the number of possible isomers exceeds a hundred thousand for fullerenes larger than C_{90}. Moreover, most of these stability models do not connect, in a straightforward way, the stability of fullerene anions to the topology of the cage. In an early attempt, Poblet et al.[33] have pointed out, based on electrostatic arguments, that pyracylene motifs are usually avoided in EMFs, especially for cages with a formal transfer of six electrons. More recently, we have demonstrated that the relative stability of charged fullerene isomers can be well understood by using the concepts of cage connectivity and frontier π orbitals.[37] On the basis of these concepts, we have proposed a pure topology-based parameter, the charge stabilization index (CSI), that allows one to correctly predict the most stable isomers of charged fullerenes, without performing geometry optimizations or iterative electronic structure calculation.[37] Nevertheless, one still needs to diagonalize the so-called adjacency matrix to apply the CSI model, which does not provide a direct visual criterion to anticipate the cage characteristics that are expected to give the largest stability.

In this article, we show that the relative stability of anionic fullerene isomers is largely governed by a few simple structural motifs. In practice, the most suitable hosting cages in EMFs can be conveniently and quantitatively predicted by merely counting the three key motifs shown in Figure 1. The predictive power of this simple model, which requires only the knowledge of the connectivity between atoms, is surprisingly good for a wide range of cage sizes in different charge states, i.e., C_{2n}^{q} ($2n$ = 68−104, q = −2, −4, −6), including both IPR and non-IPR isomers. The model also provides an explanation for why the IPR is often violated in smaller EMFs. On the basis of this model, we propose simple topological indices and rules for a rapid determination of suitable hosting cages in EMFs.

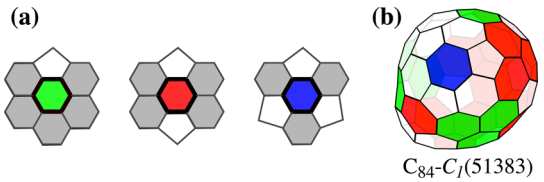

Figure 1. (a) The three key motifs that govern the stability of fullerene anions. Each motif corresponds to a central hexagon classified by the number and locations of its neighboring pentagons. Different kinds of central hexagons are indicated by different colors and highlighted with bold lines. Neighboring hexagons and pentagons are indicated by gray and white areas, respectively. (b) A fullerene structure showing the presence of these key motifs, exemplified by cage isomer C_{84}-C_1(51383), which has been experimentally identified in EMF Y_2C_2@C_{84}.[38] Only the central hexagons are indicated by their corresponding color defined in panel (a).

2. COMPUTATIONAL METHODS

All geometries and ring spiral codes of fullerene isomers were generated by the CaGe program.[39] The highest possible symmetries of fullerene isomers were identified using the fullerene database in the Fullerene program.[40] The labeling of fullerene isomers in this paper follows the conventional nomenclature[1] indicating the symmetry and the isomer number according to Fowler−Manolopoulos spiral algorithm.[41]

DFT computations at the B3LYP/6-31G(d)[42,43] level were carried out using the Gaussian 09 package.[44] The B3LYP functional has been successfully employed in many previous studies for neutral[45−47] and anionic fullerenes[32,37,48−50] as well as metallofullerenes.[48,51−55] In this work, all the experimentally identified cage isomers in EMFs have been correctly predicted as one of the lowest-energy isomers at the B3LYP/6-31G(d) level. We have also performed some additional DFT calculations with the 6-31+G(d) basis set and found that the difference in relative isomer energies between the calculations with and without diffuse functions in the basis set is typically less than ∼1 kcal/mol. Moreover, we have calculated relative energies for some systems at the MP2/6-31+G(d) level, and the results are in agreement with the DFT calculations. All details about the assessment are given in Section 1 of Supporting Information. The self-consistent charge density functional tight-binding (SCC-DFTB) calculations[56] were performed using the DFTB+ (version 1.2) code.[57] The accuracy of the SCC-DFTB method for neutral and charged fullerenes has been validated by the good agreement with the B3LYP/6-31G(d) results, as given in previous work.[37,46,58]

All total energies were computed using the equilibrium geometries which were fully optimized without any constraint. Both singlet and triplet states have been considered in the DFT calculations to determine the lowest-energy isomers. It is found that the singlet state is always more stable than the triplet for all considered systems of fullerene hexaanions. This is also true for most cases of the tetraanionic and dianionic systems. Therefore, we have only taken into account singlet states in the SCC-DFTB method due to the large number of calculations required.

To get additional chemical insight on the stabilizing behavior of the key motifs considered in this work, we have performed geometry optimizations and energy computations at the B3LYP/6-311++G(d,p) level for the corresponding polycyclic aromatic hydrocarbons (PAHs) obtained by terminating those motifs with H atoms. It has been shown that the electron affinity of coronene calculated at this level is in very good agreement with the experimental value.[59] Harmonic oscillator model of aromaticity (HOMA) indices[60] have been calculated using the optimized geometries. The curvatures of these PAHs have been calculated based on a least-squares fit of positions of carbon atoms to a spherical cap.

3. RESULTS AND DISCUSSION

3.1. Hexagon-Based Structural Motifs. There have been attempts to connect structural motifs to the stability of neutral fullerenes.[45,47,61] Austin et al.[61] have used 16 different motifs, each of which consists of two or three pentagons and/or hexagons, to analyze the total energies of the 1812 isomers of neutral C_{60}. The correlations of isomer energies with these motifs give quite scattered plots, and just some general tendencies. They also found that the correlation is much better with the second moment of the so-called hexagon-neighbor index that was originally introduced by Raghavachari.[62] On the basis of 30 distinct structural motifs, Cioslowski et al.[45] have accurately estimated the standard enthalpies of formation of 115 neutral IPR fullerenes. These motifs are hexagon based: each has a central hexagonal ring with 6−12 pentagon and/or

DOI: 10.1021/jacs.5b10591
J. Am. Chem. Soc. 2016, 138, 1551−1560

hexagon neighbors. Although this model gives an incorrect convergence toward the graphene limit, it works satisfactorily for medium-sized IPR fullerenes.[29] Very recently, Gao et al.[63] have proposed a simple rule of thumb to predict which metallofullerene multiple adducts are chemically stable. It is demonstrated that a chemically stable structure should contain isolated aromatic patches so that a large first excitation energy can be expected. These aromatic motifs must be local domains that are separated by substituent groups. Hence, it works for small-cage or low-symmetry EMFs and fullerene adducts with a large number of substituents, where the global delocalization of π-electrons is not prominent.[63]

Unlike neutral fullerenes, charged fullerenes require much fewer and simpler structural motifs to satisfactorily reproduce their relative energies, as we will show below. In this work, we have chosen the hexagon-based motifs that are related to the hexagon-neighbor indices. Here, we exclude the isomers containing triple fused pentagons[27] (TFPs, see Figure 2)

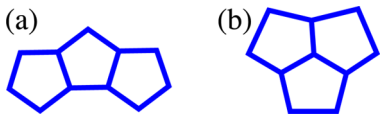

Figure 2. Triple fused pentagons: (a) Triple sequentially fused pentagons. (b) Triple directly fused pentagons.[27]

and/or more than three APPs. Such structures are highly unstable due to steric strain and thus have never been found for cage sizes larger than C_{66}, neither in the experimentally identified EMFs, nor in the computationally determined stable neutral or charged fullerenes. The only exception is the cage in EMF $Sc_2@C_{66}$,[10,21,22] which contains a pair of triple sequentially fused pentagons (see Figure 2a). The description of this special case requires a more elaborate motif model, which is discussed in Section 10 of Supporting Information. Very recently, a nonclassical fullerene cage containing a heptagonal ring has been discovered in $LaSc_2N@C_{80}$.[64] However, nonclassical fullerenes are beyond the scope of the present work and we will concentrate on classical fullerenes. Therefore, in all the isomers that we consider in this work, there are at most eight kinds of hexagon-based motifs, which are named H0, H1, H2, H2′, H2″, H3, H3′ and H4, as shown in Figure 3a. The letter H implies that these motifs are hexagon-based; each motif is uniquely associated with its central hexagon. The number following letter H indicates the number of pentagon neighbors, and the prime and double prime symbols are used to distinguish, if necessary, the motifs

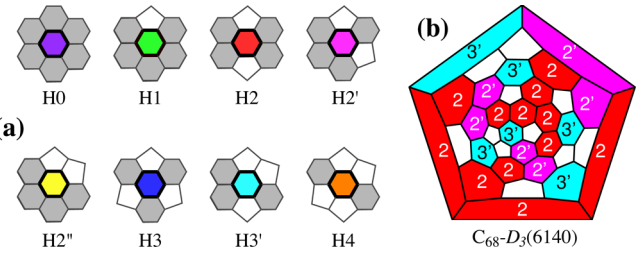

Figure 3. (a) The eight hexagon-based motifs for TFP-free fullerenes with no more than 3 APPs. The neighboring pentagons and hexagons are indicated in white and gray, respectively. See the text for the nomenclature of these motifs. (b) An example of the identification of these motifs for C_{68}-D_3(6140).[65,66]

with the same number but different locations of the neighboring pentagons. An example of the identification of these motifs is provided in Figure 3b, showing the Schlegel diagram for the C_{68}-D_3(6140) cage, which has been experimentally identified in EMFs, e.g., $Sc_3N@C_{68}$.[65,66]

The following relationships between the counts of these motifs hold for any fullerene structure C_{2n}:

$$N_0 + N_1 + N_2 + N_{2'} + N_{2''} + N_3 + N_{3'} + N_4 = n - 10 \quad (1)$$

$$N_1 + 2N_2 + 2N_{2'} + 3N_{2''} + 3N_3 + 4N_{3'} + 6N_4 = 60 \quad (2)$$

and

$$(N_{2''} + N_{3'})/2 + N_4 = \mathrm{NAPP} \quad (3)$$

where N_i is the count of motif H_i and NAPP the number of APPs. These equations are derived based on the total number of hexagons, the total number of pentagonal edges and the total number of APPs, respectively (see Section 1 of Supporting Information for more details).

3.2. Fitting the Total Energy in Terms of Seven Motifs.

We have chosen a sufficient number (hundreds or thousands, see Section 2 of Supporting Information) of isomers for each size and each charge state of fullerenes, C_{2n}^{q} ($2n$ = 68−104, q = 0, −2, −4, −6). The total energies of these isomers were calculated at the SCC-DFTB level,[56] and then were fitted using a linear combination of the energy parameters of the motifs, as formulated by the following equation:

$$E = E_0N_0 + E_1N_1 + E_2N_2 + E_{2'}N_{2'} + E_{2''}N_{2''} + E_3N_3 + E_{3'}N_{3'} \quad (4)$$

where E_i is the energy parameter of motif H_i. Note that the combination of eqs 1−3 gives rise to a linear dependence relation among the counts of motifs N_i. Because of this linear dependence, only 7 motifs are used in eq 4. Although it does not contain any term involving N_4, this equation applies to any fullerene structures with or without motif H4. We would also like to stress that the energy parameter E_i here does not correspond to the exact energy contribution of motif H_i, because of the linear dependence (see Section 4 of Supporting Information). It is assumed that E_i depends only on cage size $2n$ and charge state q, and is constant for different isomers with the same cage size and in the same charge state. We have found that E_i can be nicely reproduced using the following universal formula for all cage sizes:

$$E_i = \frac{A_i}{2n - B_i} + C_i \quad (5)$$

where parameters A_i, B_i and C_i correspond to motif H_i and are constant for all cage sizes, but depend on charge state. More detailed explanations of the linear dependence and the form of eq 5 can be found in Section 3 of Supporting Information. The fitted values of A_i, B_i and C_i for fullerene hexaanions C_{2n}^{6-} are listed in Table 1. Figure 4 shows the comparison of the relative isomer energies obtained from the fit and from the SCC-DFTB calculations for hexaanions C_{72}^{6-}, C_{78}^{6-} and C_{100}^{6-}. As we can see, not only the experimentally identified cage isomers in EMFs are well predicted to be one of the lowest-energy isomers, but also the general trends in relative isomer energies are adequately reproduced.

DOI: 10.1021/jacs.5b10591
J. Am. Chem. Soc. 2016, 138, 1551−1560

Table 1. Fitted Parameters[a] To Reproduce the SCC-DFTB Energies of C_{2n}^{6-}

i[b]	A_i (eV)	B_i	C_i (eV)
0	−3604.414	40.015	−95.150
1	−3041.971	39.888	−79.102
2	−2464.640	39.739	−62.925
2′	−2464.130	39.743	−62.838
2″	−1884.069	39.411	−46.412
3	−1869.578	39.579	−46.728
3′	−1281.097	39.167	−30.477

[a]See eq 5. [b]See Figure 3 for the notations of motifs.

The fitting results for other cage sizes and charge states are also satisfactory. Those comparisons as well as the fitted parameters can be found in Section 3 of Supporting Information. Despite its simplicity, the present seven-motif model is sufficient to reproduce nicely the relative stabilities of negatively charged fullerenes, especially hexaanions and tetraanions. In the next section, we show that the seven motifs can be practically reduced to four key motifs, which provides an even simpler picture for the stability of fullerene anions.

3.3. Key Motifs for the Relative Stability of Fullerene Anions. First, we show that stable neutral or anionic fullerenes should not contain any H4 motif. By examining all the isomers of C_{2n}^{q} ($2n$ = 68−100, q = 0, −2, −4, −6) that we have chosen, we found that the H4-containing structure is at least ∼30 kcal/mol higher in energy than the most stable isomer of neutral or anionic fullerenes (see Figure S7 of Supporting Information). This observation can be understood by the fact that the H4 substructure contains two APPs close to each other resulting in substantial strain (see Figure 3a).

Taking advantage of this conclusion, all the H4-containing structures can be safely ignored in the search for stable isomers. By setting N_4 = 0 and eliminating the terms $N_{2'}$, $N_{2''}$ and $N_{3'}$ using eqs 1−3, eq 4 can be simplified as

$$\mathcal{E} = \epsilon_0 N_0 + \epsilon_1 N_1 + \epsilon_2 N_2 + \epsilon_3 N_3 + \mathrm{NAPP} \quad (6)$$

where $\mathcal{E}$ is the relative energy and ϵ_i is the contribution to $\mathcal{E}$ from the key motif H_i. All energies are in units of energy penalty per pentagon adjacency,[67,68] which is assumed to be constant (about 20−25 kcal/mol[37,67,68]) for a given cage size and a given charge state. The key motif contributions ϵ_i are recombinations of the already fitted parameters E_i in eq 4 (see Section 8 of Supporting Information for the detailed derivation). In principle, one can also choose other sets of motifs as the key motifs, e.g., H0, H1, H2′ and H3, or H0, H1, H2 and H2′. However, as explained in detail in Section 9 of Supporting Information, the use of other sets of key motifs either does not allow to describe the structures of all isomers or provides less physical insight.

Therefore, by excluding isomers containing the H4 motif, relative isomer energies are determined by only four key motifs, namely, H0, H1, H2 and H3, plus the number of APPs. To discuss the dependence of isomer stability on these key motifs, we will focus mainly on the case of hexaanions, which have the strongest charge effect; the results for other charge states can be found in Section 5 of Supporting Information.

In Figure 5a, the energy contributions from the four key motifs in fullerene hexaanions are plotted as functions of cage size. The motif contributions in neutral fullerenes are also presented in Figure 5b for comparison. The first common feature that catches our attention is that, the H0 motif is always a highly destabilizing substructure for all cage sizes and in all charge states (see Figure S9 of Supporting Information for tetraanions and dianions). This is counterintuitive since one would expect that the H0 motif, which can be regarded as a coronene substructure, is strain-free and should thus be the most energetically favorable substructure. However, Figure 5 suggests that a stable fullerene isomer would tend to have the least number of coronene (H0) motifs. Indeed, so far, all the experimentally identified EMFs with formal 6-fold or 4-fold charge on the cage[1,2] do not contain any coronene motif. In the case of EMFs with formal two-electron transfer to the cage, most of the identified cages are coronene-free except a few ones containing only one coronene motif, e.g., Sm@C_{82}−C_{3v}(7),[69] Sm@C_{90}-C_{2v}(46)[70] and Sm@C_{94}−C_{3v}(134).[71] According to our SCC-DFTB calculations, all the coronene-containing fullerene hexaanions are at least 10 kcal/mol higher in energy than the most stable isomer (see Figure S8 of Supporting Information). Nonetheless, such an energy difference cannot completely rule out a coronene-containing isomer as a suitable hosting cage in EMFs, as the overall stability of an EMF depends also on entropic effects (due to very high temperature during the generation of EMFs) and on the cluster-cage interactions. The reason why the H0 motif is highly destabilizing is the lack of pentagonal rings, which are forced to accumulate on one side of the cage, thus favoring pentagon adjacencies. In other words, in a coronene-containing isomer the distribution of pentagons is the least uniform, which induces high strain in the structure. As shown in Figure 5, the destabilizing behavior of coronene motif is more significant for smaller cages and decreases as the cage grows, which is due to the curvature effect.[29] The coronene substructure prefers to be planar, which is not compatible with the curved shape of fullerene cages. The strain induced by this incompatibility is

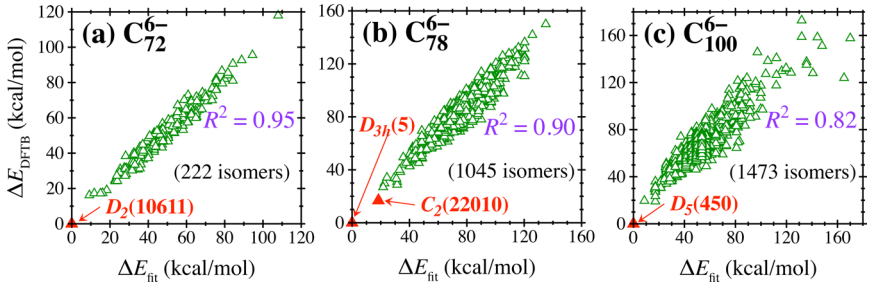

Figure 4. Comparison of relative isomer energies between the fitted values and the ones calculated at the SCC-DFTB level, exemplified by (a) C_{72}^{6-}, (b) C_{78}^{6-} and (c) C_{100}^{6-}. Total number of isomers and correlation coefficients, R^2, are given in each plot. Experimentally identified cage isomers in EMFs are marked in red and labeled[1] according to the symmetry and the isomer number given by the spiral algorithm.[41]

DOI: 10.1021/jacs.5b10591
J. Am. Chem. Soc. 2016, 138, 1551−1560

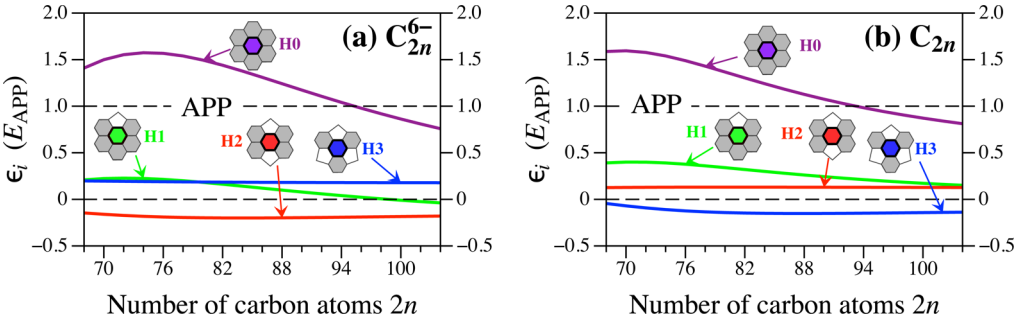

Figure 5. Energy contributions ϵ_i from the four key motifs as functions of cage size 2n, for (a) C_{2n}^{6-} and (b) C_{2n}. The dashed line indicates the energy penalty per pentagon adjacency (APP), used as the unit of energy for the plots.

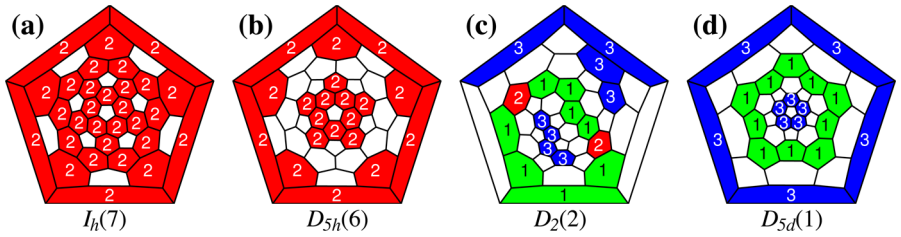

Figure 6. Schlegel diagrams for C_{80} isomers: (a) $I_h(7)$, (b) $D_{5h}(6)$, (c) $D_2(2)$ and (d) $D_{5d}(1)$. Only the key motifs are labeled and colored.

alleviated in bigger fullerenes as the cage curvature becomes smaller.

It is also interesting to see in Figure 5a that, in the case of hexaanions, the H2 motif always stabilizes the system while the H3 motif always does the opposite. The best evidence of this is provided by the most stable isomers of C_{80}^{6-}. Among all possible fullerene structures of all cage sizes, the C_{80}-$I_h(7)$ cage is the only one that has the maximum possible number of H2 motifs, namely 30, which is allowed by the icosahedral symmetry (see Figure 6a). As a result, the hexaanion C_{80}^{6-}-$I_h(7)$ should be expected to be remarkably stable. Indeed, the extraordinary stability of this hexaanion is already known; $Sc_3N@C_{80}$-$I_h(7)$[72] is the most abundant EMF ever produced and is the most abundant fullerene after C_{60} and C_{70}.[1] The second most stable isomer of C_{80}^{6-} corresponds to the $D_{5h}(6)$ cage.[28] It has the second maximum number (20) of H2 motifs (see Figure 6b), which makes it higher in energy than the $I_h(7)$ isomer (see Table 2) but still much more stable than all the other isomers of C_{80}^{6-}.

Table 2. Counts of the Key Motifs and Relative Energies (B3LYP/6-31G(d)) for the Most Stable Isomers of Hexaanions C_{80}^{6-} and Neutral C_{80}

C_{80} isomer	N_2	N_3	N_1	N_0	$E_{hexaanion}$ (kcal/mol)	$E_{neutral}$ (kcal/mol)
$I_h(7)$	30	0	0	0	0.0	27.6
$D_{5h}(6)$	20	0	0	0	23.3	10.9
$D_2(2)$	2	8	8	0	102.8	0.0
$D_{5d}(1)$	0	10	10	0	114.8	2.6

Interestingly, the stability dependence on H2 and H3 motifs is just the opposite in the neutral case: as shown in Figure 5b, the H2 motif becomes a destabilizing factor and the H3 motif a stabilizing one. Hence, one would expect that in the neutral state the above-mentioned $I_h(7)$ and $D_{5h}(6)$ isomers of C_{80} are not the most stable ones anymore, since they contain a considerable number of the energetically unfavorable H2 motifs. This qualitative reasoning is confirmed by the B3LYP/6-31G(d) calculations. As listed in Table 2, the $I_h(7)$ and $D_{5h}(6)$ neutral isomers are 27.6 and 10.9 kcal/mol, respectively, higher in energy than the most stable neutral isomer, C_{80}-$D_2(2)$. The two most stable neutral isomers, C_{80}-$D_2(2)$ and C_{80}-$D_{5d}(1)$ (they are almost degenerate in energy), have the maximum number (10) or nearly the maximum number (8) of the energetically favorable H3 motifs, respectively, as shown in Table 2 and Figure 6. On the other hand, both isomers are destabilized in the hexaanions because of the H1 and H3 motifs, being over 100 kcal/mol higher in energy than the most stable $I_h(7)$ isomer of C_{80}^{6-} (see Table 2 and Figure 6). It would be interesting to point out that Buckminsterfullerene, C_{60}-I_h, contains purely H3 motifs to achieve the maximum stability among all neutral fullerenes, in analogy to C_{80}^{6-}-I_h having purely H2 motifs which are most favorable to fullerene hexaanions.

In order to get more physical insight into the motif model, we have examined the PAHs corresponding to the key motifs (see Figure 7). Hereafter, we denote these PAH molecules as PAH-H_i, corresponding to motifs H_i (i = 0–3). As we have demonstrated recently,[37] electronic and strain effects are the two key factors determining stability of charged fullerenes. Here, we show that the stabilization effects of motifs can also be understood by the interplay of these two factors.

First, it is found that PAH-H2 has the highest electron affinity (2.42 eV) while PAH-H3 has a much lower value (1.89 eV). This indicates that the H2 motif is a much better electron acceptor than H3, which is in line with the conclusion that the former is more stabilizing than the latter in fullerene hexaanions. Meanwhile, PAH-H1 also has nearly the same value of electron affinity (2.40 eV) as that of PAH-H2. However, the H1 motif is energetically less favorable than H2, especially for small cages. This can be explained by curvature effect. As shown in Figure 7, PAH-$H1^-$ monoanion has a planar structure, which is not compatible with the curved shape of fullerene cages and thus induces considerable local strain when integrated into a fullerene cage. Therefore, despite of being a

DOI: 10.1021/jacs.5b10591
J. Am. Chem. Soc. 2016, 138, 1551–1560

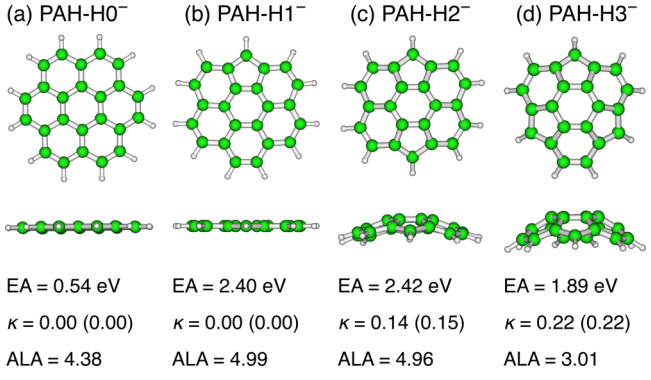

Figure 7. Top (upper row) and side (middle row) views of the optimized geometry of PAH monoanions corresponding to motifs H0, H1, H2 and H3. First adiabatic electron affinity (EA) of neutral PAHs, curvature (κ, in Å^{-1}) and ALA index of monoanionic PAHs, calculated at the B3LYP/6-311++G(d,p) level, are given at the bottom. The curvature for neutral PAHs is provided in parentheses.

good electron acceptor, H1 motif is still destabilizing for small cages. When the cage is larger, this curvature effect is smaller and the H1 motif becomes more stabilizing, as can be seen in Figure 5a. In comparison, PAH-H2$^-$ and PAH-H3$^-$ have a curved structure (the curvatures being 0.14 and 0.22 Å^{-1}, respectively), which is compatible with the curved cage shape (e.g., the curvature of C_{80}^{6-}-I_h(7) is 0.24 Å^{-1}). In the case of PAH-H0, it is planar and has low electron affinity (0.54 eV). Both factors explain why the H0 motif is highly destabilizing.

Since Solà et al.[35,36] have found that aromaticity plays a key role in the stability of EMFs, we have also examined the aromaticities of these PAHs. The aromaticity has been evaluated by the additive local aromaticity (ALA) index,[35,36] defined as the sum of the local aromaticities of all rings in the PAH molecule. The ALA has been calculated in terms of the HOMA index,[60] which has been shown to be able to predict the isomer stability of charged fullerenes.[35,36] As shown in Figure 7, monoanion PAH-H2$^-$ is much more aromatic (ALA = 4.96) than PAH-H3$^-$ (ALA = 3.01), consistent with the fact that the former motif is stabilizing and the latter destabilizing. Although monoanion PAH-H1$^-$ is as aromatic as PAH-H2$^-$ (ALA = 4.99), the H1 motif is still less stabilizing than H2 because of the above-mentioned curvature effect.

In the case of neutral fullerenes, as pointed out by Solà and co-workers,[35,36] aromaticity plays no role in the relative stability of different isomers and instead strain is the dominant factor. As shown in Figure 7, neutral PAH-H3 has a curvature (0.22 Å^{-1}) very similar to that of fullerene cages (ranging from 0.20 to 0.22 Å^{-1} for C_{70} to C_{100}), which explains why H3 is the most stabilizing motif for neutral fullerenes. In comparison, PAH-H2 has a less compatible curvature (0.15 Å^{-1}) and thus the H2 motif is energetically less favorable. For the same reason, H0 and H1 are the most destabilizing motifs for neutral fullerenes due to their planar structure.

It is worth mentioning that the H3 motif has three pyracylenic substructures while H2 has none. This also explains why the latter is more energetically favorable than the former since the presence of pyracylene units has been associated with strong Coulomb repulsion.[30]

3.4. An Explanation for the Violation of IPR in EMFs.

One of the puzzling facts about EMFs is the frequent appearance of non-IPR structures.[1,27] DFT calculations[28] have revealed that the non-IPR isomers are more stable than the IPR ones for fullerene hexaanions no larger than C_{84}^{6-}. However, the non-IPR hexaanions become more and more unstable as the cage size increases. As a consequence, beyond C_{84}^{6-} the non-IPR isomers cannot compete in stability with the IPR ones, and thus the IPR remains valid again. Here, we provide an explanation of this interesting observation in terms of the key motifs.

In an IPR isomer of smaller fullerenes, hexagons are mostly used to separate all 12 pentagons. As a result, there are fewer H2 and more H3 motifs, since the former requires four hexagon neighbors and the latter requires only three. In contrast, without the constraint that all pentagons must be isolated, in a non-IPR isomer the hexagons are free to form as many H2 motifs, and as few H3 motifs, as possible. Since the former motif is stabilizing and the latter destabilizing for fullerene hexaanions, a non-IPR isomer can be more stable than

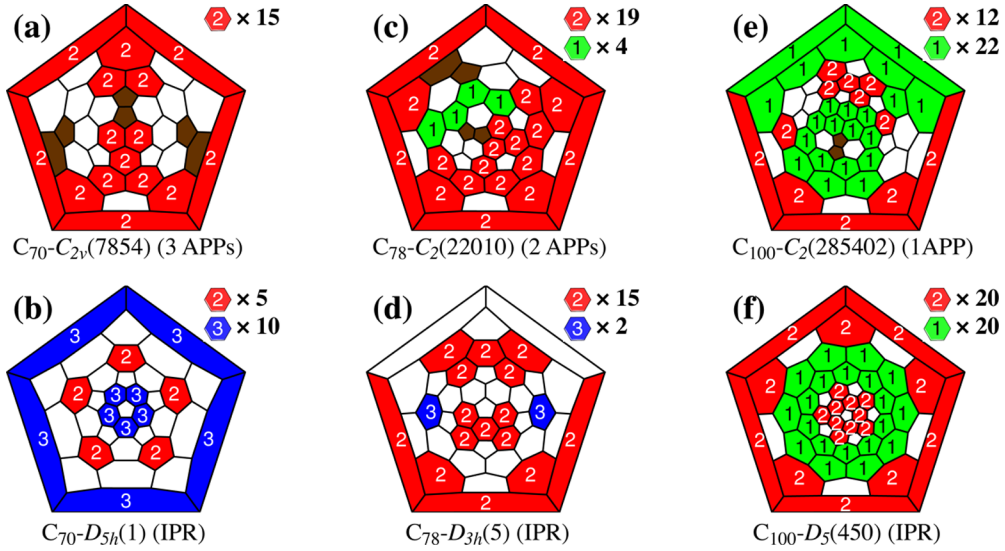

Figure 8. Schlegel diagrams for the lowest-energy non-IPR and IPR isomers of C_{70}^{6-}, C_{78}^{6-} and C_{100}^{6-}. Only the key motifs H1, H2 and H3 are labeled and colored. APPs are colored in brown. The number of APPs are given in parentheses following the isomer label. The counts of the key motifs are indicated at the upper right corner of each panel.

DOI: 10.1021/jacs.5b10591
J. Am. Chem. Soc. 2016, 138, 1551−1560

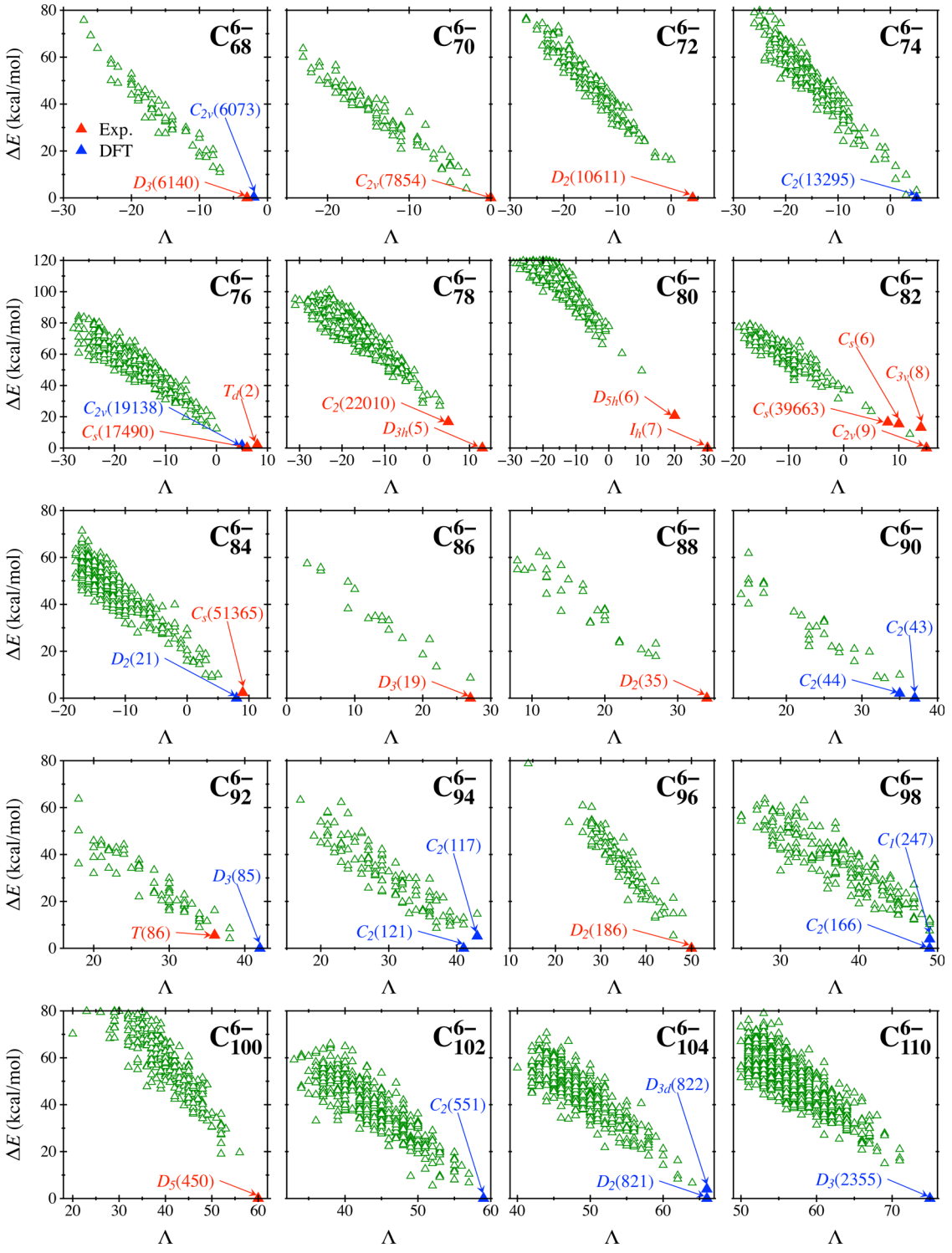

Figure 9. Correlation between Λ (using eq 7) and the relative isomer energy at the SCC-DFTB level for C_{2n}^{6-} hexaanions. The cage structures that have been experimentally identified in EMFs are labeled and marked in red. The lowest-energy isomers of hexaanions determined by DFT are labeled and marked in blue.

an IPR one. An example is given in Figure 8a and b, showing the structures of the lowest-energy non-IPR and IPR isomers of C_{70}^{6-}, $C_{2v}(7854)$ and $D_{5h}(1)$, respectively. The former has much more H2 and fewer H3 motifs than the latter so that the motif stabilization takes over the pentagon adjacency penalty. Consequently, the non-IPR $C_{2v}(7854)$ is the most stable isomer of C_{70}^{6-}.

The situation changes when the cage becomes larger. The increasing number of hexagons allows an IPR isomer to form more hexagon-rich H2 motifs and fewer hexagon-poor H3 motifs. This tendency can be seen in Figure 8. The number of the H2 motifs increases from 5 to 15 when the cage enlarges from C_{70}-$D_{5h}(1)$ (Figure 8b) to C_{78}-$D_{3h}(5)$ (Figure 8d), and in C_{100}-$D_5(450)$ (Figure 8f) there are as many as 20 H2 motifs. Meanwhile, there are 10 H3 motifs in C_{70}-$D_{5h}(1)$, whereas this

DOI: 10.1021/jacs.5b10591
J. Am. Chem. Soc. 2016, 138, 1551−1560

number decreases to 2 in C_{78}-$D_{3h}(5)$ and drops to zero in C_{100}-$D_5(450)$. Thus, the increasing number of H2 motifs in parallel with the decrease of H3 motifs makes the IPR hexaanions more stable as the cage becomes larger. This explains why the IPR is valid again for the larger fullerene hexaanions.

It is worth noticing that the H1 motifs only start to appear when the fullerene cage is large enough, as shown in Figure 8c, e and f. But this motif becomes more dominant than the H2 motif only when the cage is larger than C_{94} (see Table S5 of Supporting Information). At such sizes, the numbers of H1 motifs in the lowest-energy non-IPR and IPR isomers are similar (see Figure 8e and f, and Table S5 of Supporting Information). Therefore, the inclusion of H1 motifs does not affect the discussions presented above.

3.5. Simple Topological Index and Rules for Rapid Determination of Suitable Hosting Cages in EMFs. First, we show that, for determining the relative stability of fullerene hexaanions and tetraanions, the aforementioned four key motifs can be practically reduced to three. For cage sizes from C_{68} to C_{84}, as demonstrated in Section 3.3, the coronene-containing isomers of hexaanions and tetraanions are at least 30 and 20 kcal/mol, respectively, higher in energy than the most stable isomer (see Figure S8 of Supporting Information). Hence, the isomers containing H0 motifs can be ruled out in the search for stable hexaanions and tetraanions. This reduces the four key motifs to three motifs, H1, H2 and H3. Similarly, for cages larger than C_{84}, the IPR is applicable again, as discussed in the previous section, so that the number of the key motifs can also be reduced to three (see Section 7 of Supporting Information).

On the basis of the average energy contributions from the three motifs, H1, H2 and H3, we propose the following topological index, Λ, for the relative stability of fullerene hexaanions:

$$\Lambda \equiv \begin{cases} N_2 - N_3 - N_1 - 5 & \text{from } C_{68}^{6-} \text{ to } C_{84}^{6-} \\ \quad \text{NAPP} & \text{(coronene-free)} \\ N_2 - 4N_3 + 2N_1 & \text{beyond } C_{84}^{6-} \text{ (IPR)} \end{cases} \quad (7)$$

The coefficients in the formula of Λ are simple integers that are approximately proportional to the average values of motif contributions in a given range of cage sizes (see the derivation in Section 8 of Supporting Information). A large value of Λ indicates a higher stability of the hexaanion. There is a good correlation between Λ and the relative energies obtained from the SCC-DFTB calculations. As can be seen in Figure 9, the Λ index works well for cage sizes from C_{68} up to, at least, C_{110}. It is able to predict all experimentally identified cage structures in EMFs, as well as the lowest-energy isomers of hexaanions determined by DFT and the relative isomer stability for a given size. It is worth mentioning that the topological index also works very well for metal intercalated fullerides, such as Li_6C_{60},[73] Na_6C_{60},[74] K_6C_{60},[75,76] Ba_3C_{60},[77] where the cage can be regarded as a hexaanion (see Section 8 of Supporting Information).

For fullerene tetraanions, a similar topological index is proposed as follows,

$$\Lambda \equiv \begin{cases} N_2 - N_3 - 2N_1 - 10\text{NAPP} & \text{from } C_{68}^{4-} \text{ to } C_{84}^{4-} \\ & \text{(coronene-free)} \\ N_2 - 5N_3 + 4N_1 & \text{beyond } C_{84}^{4-} \text{ (IPR)} \end{cases} \quad (8)$$

which also correlates nicely with the relative energies of tetraanions. We have also proposed a topological index for dianions. Although the prediction power is worse than for hexaanions and tetraanions, it can still be used as a rule of thumb to roughly estimate the relative isomer stability (see Section 7 of Supporting Information).

Finally, we would like to summarize the topological rules for a rapid determination of the preferred hosting cages in EMFs (from C_{68} up to, at least, C_{110}), as follows: (i) A suitable hosting cage should not have any TFPs or more than three APPs. (ii) It should have no H4 motifs. (iii) It tends to avoid having H0 (coronene) motifs. Only a few exceptions have been found in EMFs with formal two- or three-electron transfer to the cage, where the cage contains only one H0 motif. (iv) The IPR is valid for all sizes of the EMFs with formal two- or three-electron transfer to the cage, and for large EMFs (beyond C_{84}) with formal four- or six-electron transfer. In all other cases, non-IPR structures are likely to be the most stable ones and consequently must be considered.

The above rules can screen out a significant number of candidates in the search for suitable cages in EMFs or in fullerene anions. Thereafter, by counting the numbers of H1, H2 and H3 motifs and calculating the corresponding topological indices, the relative stability of the candidate isomers can be quantitatively predicted.

4. CONCLUSIONS

On the basis of a large number of SCC-DFTB computations, we have demonstrated that the relative isomer energies of fullerene anions can be satisfactorily reproduced by merely counting the numbers of seven kinds of hexagon-based motifs. Using the linear decomposition of the total energy and the relationships among the counts of motifs, we have determined four key structural motifs that mainly govern the stability of fullerene anions. The stabilizing and destabilizing effects of the key motifs vary with the charge state, which reflects the fact that the most stable isomeric forms in EMFs often differs from those of neutral empty fullerenes. On the basis of this motif model, the violation of the IPR in small-sized EMFs can be understood. Finally, we have proposed simple topological indices for quantitatively predicting the relative isomer stability of fullerene anions. As a very practical predictor, our topological index is solely based on the counts of three simple motifs, requiring only the connectivity information between carbon atoms in the cage.

As demonstrated in Supporting Information, the present model can be easily extended to incorporate additional motifs. The extended model allows us to understand special cases, such as EMF $Sc_2@C_{66}$,[10,21,22] which contains triple sequentially fused pentagons (see Figure 2a). In short, the motif method can be applied to a wide variety of metallofullerenes and should be very useful for a broad range of scientists not familiar with quantum chemistry calculations.

■ ASSOCIATED CONTENT

Supporting Information

The Supporting Information is available free of charge on the ACS Publications website at DOI: 10.1021/jacs.5b10591.

Assessment of the DFT and SCC-DFTB methods employed in this work; relationships between the counts of the motifs; number of isomers included in the fit; fitting results for all cage sizes and charge states; relative

DOI: 10.1021/jacs.5b10591
J. Am. Chem. Soc. 2016, 138, 1551−1560

energies of the isomers containing H4 or H0 motifs; derivation of the 4-motif equation; lists of the lowest-energy IPR and non-IPR isomers of fullerene hexaanions; derivation of the simple topological indices; topological indices based on other sets of motifs; extended model for C_{66}^{6-}; summary of experimentally identified EMFs; absolute energies and optimized geometries of the most stable isomers of C_{80}^{6-} and C_{80}. (PDF)

AUTHOR INFORMATION

Corresponding Author

*yang.wang@uam.es

Notes

The authors declare no competing financial interest.

ACKNOWLEDGMENTS

We acknowledge allocation of computer time at the Centro de Computación Científica at the Universidad Autónoma de Madrid (CCC-UAM). Work supported by the MINECO projects FIS2013-42002-R, CTQ2013-43698-P and FIS2013-40667-P, the CAM project NANOFRONTMAG-CM (ref S2013/MIT-2850), and the European COST Action CM1204 XLIC. S. D.-T. acknowledges the "Ramón y Cajal" program.

REFERENCES

(1) Popov, A. A.; Yang, S.; Dunsch, L. *Chem. Rev.* **2013**, *113*, 5989−6113.

(2) Lu, X.; Feng, L.; Akasaka, T.; Nagase, S. *Chem. Soc. Rev.* **2012**, *41*, 7723−7760.

(3) Akasaka, T.; Lu, X. *Chem. Rec.* **2012**, *12*, 256−269.

(4) Dorn, H. C.; Fatouros, P. P. *Nanosci. Nanotechnol. Lett.* **2010**, *2*, 65−72.

(5) Anilkumar, P.; Lu, F.; Cao, L.; Luo, P. G.; Liu, J.-H.; Sahu, S.; Tackett, K. N., II; Wang, Y.; Sun, Y.-P. *Curr. Med. Chem.* **2011**, *18*, 2045−2059.

(6) Chen, Z.; Mao, R.; Liu, Y. *Curr. Drug Metab.* **2012**, *13*, 1035−1045.

(7) Rudolf, M.; Wolfrum, S.; Guldi, D. M.; Feng, L.; Tsuchiya, T.; Akasaka, T.; Echegoyen, L. *Chem. - Eur. J.* **2012**, *18*, 5136−5148.

(8) Ross, R. B.; Cardona, C. M.; Guldi, D. M.; Sankaranarayanan, S. G.; Reese, M. O.; Kopidakis, N.; Peet, J.; Walker, B.; Bazan, G. C.; Van Keuren, E.; Holloway, B. C.; Drees, M. *Nat. Mater.* **2009**, *8*, 208−212.

(9) Takata, M.; Umeda, B.; Nishibori, E.; Sakata, M.; Saitot, Y.; Ohno, M.; Shinohara, H. *Nature* **1995**, *377*, 46−49.

(10) Wang, C.-R.; Kai, T.; Tomiyama, T.; Yoshida, T.; Kobayashi, Y.; Nishibori, E.; Takata, M.; Sakata, M.; Shinohara, H. *Nature* **2000**, *408*, 426−427.

(11) Wang, Z.; Nakanishi, Y.; Noda, S.; Niwa, H.; Zhang, J.; Kitaura, R.; Shinohara, H. *Angew. Chem., Int. Ed.* **2013**, *52*, 11770−11774.

(12) Kurihara, H.; Lu, X.; Iiduka, Y.; Nikawa, H.; Mizorogi, N.; Slanina, Z.; Tsuchiya, T.; Nagase, S.; Akasaka, T. *J. Am. Chem. Soc.* **2012**, *134*, 3139−3144.

(13) Lu, X.; Nakajima, K.; Iiduka, Y.; Nikawa, H.; Tsuchiya, T.; Mizorogi, N.; Slanina, Z.; Nagase, S.; Akasaka, T. *Angew. Chem., Int. Ed.* **2012**, *51*, 5889−5892.

(14) Suzuki, M.; Slanina, Z.; Mizorogi, N.; Lu, X.; Nagase, S.; Olmstead, M. M.; Balch, A. L.; Akasaka, T. *J. Am. Chem. Soc.* **2012**, *134*, 18772−18778.

(15) Zhang, W.; Suzuki, M.; Xie, Y.; Bao, L.; Cai, W.; Slanina, Z.; Nagase, S.; Xu, M.; Akasaka, T.; Lu, X. *J. Am. Chem. Soc.* **2013**, *135*, 12730−12735.

(16) Dresselhaus, M.; Dresselhaus, G.; Eklund, P. *Science of Fullerenes and Carbon Nanotubes*; Academic Press: New York, 1996.

(17) Dunk, P. W.; Kaiser, N. K.; Mulet-Gas, M.; Rodríguez-Fortea, A.; Poblet, J. M.; Shinohara, H.; Hendrickson, C. L.; Marshall, A. G.; Kroto, H. W. *J. Am. Chem. Soc.* **2012**, *134*, 9380−9389.

(18) Mercado, B.; Jiang, A.; Yang, H.; Wang, Z.; Jin, H.; Liu, Z.; Olmstead, M.; Balch, A. *Angew. Chem., Int. Ed.* **2009**, *48*, 9114−9116.

(19) Dunk, P. W.; Mulet-Gas, M.; Nakanishi, Y.; Kaiser, N. K.; Rodríguez-Fortea, A.; Shinohara, H.; Poblet, J. M.; Marshall, A. G.; Kroto, H. W. *Nat. Commun.* **2014**, *5*, 5844.

(20) Mulet-Gas, M.; Abella, L.; Dunk, P. W.; Rodriguez-Fortea, A.; Kroto, H. W.; Poblet, J. M. *Chem. Sci.* **2015**, *6*, 675−686.

(21) Takata, M.; Nishibori, E.; Sakata, M.; R-Wang, C.; Shinohara, H. *Chem. Phys. Lett.* **2003**, *372*, 512−518.

(22) Yamada, M.; Kurihara, H.; Suzuki, M.; Guo, J. D.; Waelchli, M.; Olmstead, M. M.; Balch, A. L.; Nagase, S.; Maeda, Y.; Hasegawa, T.; Lu, X.; Akasaka, T. *J. Am. Chem. Soc.* **2014**, *136*, 7611−7614.

(23) Diederich, F.; Whetten, R. L.; Thilgen, C.; Ettl, R.; Chao, I.; Alvarez, M. M. *Science* **1991**, *254*, 1768−1770.

(24) Kikuchi, K.; Nakahara, N.; Wakabayashi, T.; Suzuki, S.; Shiromaru, H.; Miyake, Y.; Saito, K.; Ikemoto, I.; Kainosho, M.; Achiba, Y. *Nature* **1992**, *357*, 142−145.

(25) Taylor, R.; Langley, G. J.; Dennis, T. J. S.; Kroto, H. W.; Walton, D. R. M. *J. Chem. Soc., Chem. Commun.* **1992**, 1043−1046.

(26) Kroto, H. W. *Nature* **1987**, *329*, 529−531.

(27) Tan, Y.-Z.; Xie, S.-Y.; Huang, R.-B.; Zheng, L.-S. *Nat. Chem.* **2009**, *1*, 450−460.

(28) Popov, A. A.; Dunsch, L. *J. Am. Chem. Soc.* **2007**, *129*, 11835−11849.

(29) Schwerdtfeger, P.; Wirz, L. N.; Avery, J. *WIREs Comput. Mol. Sci.* **2015**, *5*, 96−145.

(30) Campanera, J. M.; Bo, C.; Poblet, J. M. *Angew. Chem., Int. Ed.* **2005**, *44*, 7230−7233.

(31) Valencia, R.; Rodríguez-Fortea, A.; Poblet, J. M. *J. Phys. Chem. A* **2008**, *112*, 4550−4555.

(32) Zettergren, H.; Alcamí, M.; Martín, F. *ChemPhysChem* **2008**, *9*, 861−866.

(33) Rodríguez-Fortea, A.; Alegret, N.; Balch, A. L.; Poblet, J. M. *Nat. Chem.* **2010**, *2*, 955−961.

(34) Alegret, N.; Mulet-Gas, M.; Aparicio-Anglès, X.; Rodríguez-Fortea, A.; Poblet, J. M. *C. R. Chim.* **2012**, *15*, 152−158.

(35) Garcia-Borràs, M.; Osuna, S.; Swart, M.; Luis, J. M.; Solà, M. *Angew. Chem., Int. Ed.* **2013**, *52*, 9275−9278.

(36) Garcia-Borràs, M.; Osuna, S.; Luis, J. M.; Swart, M.; Solà, M. *Chem. Soc. Rev.* **2014**, *43*, 5089−5105.

(37) Wang, Y.; Díaz-Tendero, S.; Alcamí, M.; Martín, F. *Nat. Chem.* **2015**, *7*, 927−934.

(38) Zhang, J.; Fuhrer, T.; Fu, W.; Ge, J.; Bearden, D. W.; Dallas, J.; Duchamp, J.; Walker, K.; Champion, H.; Azurmendi, H.; Harich, K.; Dorn, H. C. *J. Am. Chem. Soc.* **2012**, *134*, 8487−8493.

(39) Brinkmann, G.; Friedrichs, O. D.; Lisken, S.; Peeters, A.; Cleemput, N. V. *MATCH Commun. Math. Comput. Chem.* **2010**, *63*, 533−552.

(40) Schwerdtfeger, P.; Wirz, L.; Avery, J. *J. Comput. Chem.* **2013**, *34*, 1508−1526.

(41) Fowler, P.; Manolopoulos, D. E. *An Atlas of Fullerenes*; Clarendon Press: Oxford, U.K., 1995.

(42) Lee, C.; Yang, W.; Parr, R. G. *Phys. Rev. B: Condens. Matter Mater. Phys.* **1988**, *37*, 785−789.

(43) Becke, A. D. *J. Chem. Phys.* **1993**, *98*, 5648−5652.

(44) Frisch, M. J.; Trucks, G. W.; Schlegel, H. B.; Scuseria, G. E.; Robb, M. A.; Cheeseman, J. R.; Scalmani, G.; Barone, V.; Mennucci, B.; Petersson, G. A.; Nakatsuji, H.; Caricato, M.; Li, X.; Hratchian, H. P.; Izmaylov, A. F.; Bloino, J.; Zheng, G.; Sonnenberg, J. L.; Hada, M.; Ehara, M.; Toyota, K.; Fukuda, R.; Hasegawa, J.; Ishida, M.; Nakajima, T.; Honda, Y.; Kitao, O.; Nakai, H.; Vreven, T.; Montgomery, J. A.Jr.; Peralta, J. E.; Ogliaro, F.; Bearpark, M.; Heyd, J. J.; Brothers, E.; Kudin, K. N.; Staroverov, V. N.; Keith, T.; Kobayashi, R.; Normand, J.; Raghavachari, K.; Rendell, A.; Burant, J. C.; Iyengar, S. S.; Tomasi, J.; Cossi, M.; Rega, N.; Millam, J. M.; Klene, M.; Knox, J. E.; Cross, J. B.; Bakken, V.; Adamo, C.; Jaramillo, J.; Gomperts, R.; Stratmann, R. E.; Yazyev, O.; Austin, A. J.; Cammi, R.; Pomelli, C.; Ochterski, J. W.; Martin, R. L.; Morokuma, K.; Zakrzewski, V. G.; Voth, G. A.; Salvador, P.; Dannenberg, J. J.; Dapprich, S.; Daniels, A. D.; Farkas, O.;

DOI: 10.1021/jacs.5b10591
J. Am. Chem. Soc. 2016, 138, 1551−1560

Foresman, J. B.; Ortiz, J. V.; Cioslowski, J.; Fox, D. J. *Gaussian 09*, Revision C.01; Gaussian, Inc.: Wallingford, CT, 2010.
(45) Cioslowski, J.; Rao, N.; Moncrieff, D. *J. Am. Chem. Soc.* **2000**, *122*, 8265−8270.
(46) Zheng, G.; Irle, S.; Morokuma, K. *Chem. Phys. Lett.* **2005**, *412*, 210−216.
(47) Alcamí, M.; Sánchez, G.; Díaz-Tendero, S.; Wang, Y.; Martín, F. *J. Nanosci. Nanotechnol.* **2007**, *7*, 1329−1338.
(48) Cui, Y.-H.; Tian, W. Q.; Feng, J.-K.; Chen, D.-L. *J. Comput. Chem.* **2008**, *29*, 2623−2630.
(49) Zettergren, H.; Alcamí, M.; Martín, F. *Phys. Rev. A: At., Mol., Opt. Phys.* **2007**, *76*, 043205.
(50) Wang, Y.; Zettergren, H.; Alcamí, M.; Martí, F. *Phys. Rev. A: At., Mol., Opt. Phys.* **2009**, *80*, 033201.
(51) Yumura, T.; Sato, Y.; Suenaga, K.; Iijima, S. *J. Phys. Chem. B* **2005**, *109*, 20251−20255.
(52) Popov, A. A.; Dunsch, L. *J. Am. Chem. Soc.* **2008**, *130*, 17726−17742.
(53) Slanina, Z.; Uhlík, F.; Lee, S.-L.; Adamowicz, L.; Akasaka, T.; Nagase, S. *Int. J. Quantum Chem.* **2011**, *111*, 2712−2718.
(54) Kobayashi, K.; Nagase, S. *Mol. Phys.* **2003**, *101*, 249−254.
(55) Miyazaki, T.; Okita, S.; Ohta, T.; Yagi, H.; Sumii, R.; Okimoto, H.; Ito, Y.; Shinohara, H.; Hino, S. *Chem. Phys.* **2015**, *447*, 71−75.
(56) Elstner, M.; Porezag, D.; Jungnickel, G.; Elsner, J.; Haugk, M.; Frauenheim, T.; Suhai, S.; Seifert, G. *Phys. Rev. B: Condens. Matter Mater. Phys.* **1998**, *58*, 7260−7268.
(57) Aradi, B.; Hourahine, B.; Frauenheim, T. *J. Phys. Chem. A* **2007**, *111*, 5678−5684.
(58) Wang, Y.; Zettergren, H.; Rousseau, P.; Chen, T.; Gatchell, M.; Stockett, M. H.; Domaracka, A.; Adoui, L.; Huber, B. A.; Cederquist, H.; Alcamí, M.; Martín, F. *Phys. Rev. A: At., Mol., Opt. Phys.* **2014**, *89*, 062708.
(59) Abouaf, R.; Díaz-Tendero, S. *Phys. Chem. Chem. Phys.* **2009**, *11*, 5686−5694.
(60) Kruszewski, J.; Krygowski, T. *Tetrahedron Lett.* **1972**, *13*, 3839−3842.
(61) Austin, S. J.; Fowler, P. W.; Manolopoulos, D. E.; Orlandi, G.; Zerbetto, F. *J. Phys. Chem.* **1995**, *99*, 8076−8081.
(62) Raghavachari, K. *Chem. Phys. Lett.* **1992**, *190*, 397−400.
(63) Gao, X.; Chen, B.-Z.; Gao, X. *Carbon* **2016**, *96*, 980−986.
(64) Zhang, Y.; Ghiassi, K. B.; Deng, Q.; Samoylova, N. A.; Olmstead, M. M.; Balch, A. L.; Popov, A. A. *Angew. Chem., Int. Ed.* **2015**, *54*, 495−499.
(65) Stevenson, S.; Fowler, P. W.; Heine, T.; Duchamp, J. C.; Rice, G.; Glass, T.; Harich, K.; Hajdu, E.; Bible, R.; Dorn, H. C. *Nature* **2000**, *408*, 427−428.
(66) Olmstead, M. M.; Lee, H. M.; Duchamp, J. C.; Stevenson, S.; Marciu, D.; Dorn, H. C.; Balch, A. L. *Angew. Chem., Int. Ed.* **2003**, *42*, 900−903.
(67) Campbell, E.; Fowler, P.; Mitchell, D.; Zerbetto, F. *Chem. Phys. Lett.* **1996**, *250*, 544−548.
(68) Albertazzi, E.; Domene, C.; Fowler, P. W.; Heine, T.; Seifert, G.; Van Alsenoy, C.; Zerbetto, F. *Phys. Chem. Chem. Phys.* **1999**, *1*, 2913−2918.
(69) Yang, H.; Jin, H.; Wang, X.; Liu, Z.; Yu, M.; Zhao, F.; Mercado, B. Q.; Olmstead, M. M.; Balch, A. L. *J. Am. Chem. Soc.* **2012**, *134*, 14127−14136.
(70) Yang, H.; Jin, H.; Zhen, H.; Wang, Z.; Liu, Z.; Beavers, C. M.; Mercado, B. Q.; Olmstead, M. M.; Balch, A. L. *J. Am. Chem. Soc.* **2011**, *133*, 6299−6306.
(71) Jin, H.; Yang, H.; Yu, M.; Liu, Z.; Beavers, C. M.; Olmstead, M. M.; Balch, A. L. *J. Am. Chem. Soc.* **2012**, *134*, 10933−10941.
(72) Stevenson, S.; Rice, G.; Glass, T.; Harich, K.; Cromer, F.; Jordan, M. R.; Craft, J.; Hadju, E.; Bible, R.; Olmstead, M. M.; Maitra, K.; Fisher, A. J.; Balch, A. L.; Dorn, H. C. *Nature* **1999**, *401*, 55−57.
(73) Gaboardi, M.; Duyker, S.; Milanese, C.; Magnani, G.; Peterson, V. K.; Pontiroli, D.; Sharma, N.; Riccò, M. *J. Phys. Chem. C* **2015**, *119*, 19715−19721.
(74) Yildirim, T.; Zhou, O.; Fischer, J. E.; Bykovetz, N.; Strongin, R. A.; Cichy, M. A.; Smith, A. B., III; Lin, C. L.; Jelinek, R. *Nature* **1992**, *360*, 568−571.
(75) Zhou, O.; Fischer, J. E.; Coustel, N.; Kycia, S.; Zhu, Q.; McGhie, A. R.; Romanow, W. J.; McCauley, J. P.; Smith, A. B.; Cox, D. E. *Nature* **1991**, *351*, 462−464.
(76) Allen, K. M.; David, W. I. F.; Fox, J. M.; Ibberson, R. M.; Rosseinsky, M. J. *Chem. Mater.* **1995**, *7*, 764−770.
(77) Knupfer, M.; Stepniak, F.; Weaver, J. H. *Phys. Rev. B: Condens. Matter Mater. Phys.* **1994**, *49*, 7620−7624.

DOI: 10.1021/jacs.5b10591
J. Am. Chem. Soc. 2016, 138, 1551−1560